J|A|C|S
ARTICLES
Published on Web 10/05/2004

Single-Molecule Spectroscopy Studies of Microenvironmental Acidity in Silicate Thin Films

Yi Fu, Maryanne M. Collinson,* and Daniel A. Higgins*

Contribution from the Department of Chemistry, Kansas State University, Manhattan, Kansas 66506

Received June 11, 2004; E-mail: mmc@ksu.edu; higgins@ksu.edu

Abstract: Single-molecule (SM) spectroscopic methods were employed to study single site variations in the acidity properties of sol−gel-derived silicate films. The pH-sensitive dye Carboxy SNARF-1 (C.SNARF-1) was used to sense film acidity. Its concentration in the films was maintained at nanomolar levels to allow for SMs to be spectroscopically interrogated. The ratio of C.SNARF-1 fluorescence at 580 nm (protonated form) and 640 nm (deprotonated form) was used to characterize local film pH. SM data were acquired both for "untreated" films and for those treated by immersion for either 1 or 8 h in phosphate solutions of different pH. The SM results prove that the spectral variability observed is dominated by static variations in the local matrix acidity. Shorter immersion times lead to relatively broad histograms and broad "titration" curves, providing clear evidence for kinetic limitations to access of certain film environments by the immersion solutions. Films subjected to longer immersion times generally exhibit narrower histograms. Particularly narrow distributions were obtained for films treated near pH 8−9, while much broader histograms were produced near pH 7. These results are attributed to the buffering effects of surface silanols near pH 9 and enhanced pH sensitivity of the dye near pH 7.

Introduction

A better understanding of the local microenvironments within sol−gel-derived silicates is of great importance to the design of advanced materials with potential applications as chemical sensors,[1−3] photonic devices,[4−6] catalysts,[7,8] catalytic supports,[9] and in separations.[10] It is well known that a significant number of acidic sites exist on the surfaces of "pure" silicate films. Surface site acidity is mostly due to the presence of silanol groups (Si−OH).[11] These weakly acidic silanols play an important role in governing the chemistry of molecule−matrix interactions. For instance, surface silanols participate directly in the chemisorption of polar molecules via hydrogen bonding and/or ionic species via electrostatic interactions.[11−14] They are also involved in a number of relevant catalytic reactions.[7,8] Importantly, their overall properties (i.e., whether they are protonated or deprotonated) are also strongly influenced by the presence of residual catalyst (acid or base) employed during sol−gel synthesis. The acidity properties of silica materials have been studied by methods such as temperature-programmed desorption (TPD),[15,16] FTIR,[17,18] and NMR spectroscopy.[15,16] Such methods provide valuable information on the average acidity of the relevant surface sites. While the observation of broad spectral peaks is indicative of sample heterogeneity, the origins of and length scales over which variations in surface site acidity occur are difficult to determine by such methods. It is also impossible to fully understand the properties of the individual sites that define the local surface acidity by bulk methods alone. Therefore, new methodologies that provide direct information on the acidity properties of single microenvironments in sol−gel-derived silicates need to be established.

Single-molecule (SM) spectroscopy has recently emerged as a valuable means for directly probing the properties of local environments in a wide variety of materials.[19−25] In these methods, dyes sensitive to specific environmental properties are doped into the sample of interest at very low (i.e., nanomolar)

(1) Lin, J.; Brown, C. W. *Trends Anal. Chem.* **1997**, *16*, 200.
(2) Dave, B. C.; Dunn, B.; Valentine, J. S.; Zink, J. I. *Anal. Chem.* **1994**, *66*, 1120A.
(3) Lev, O.; Tsionsky, M.; Rabinovich, L.; Glezer, V.; Sampath, S.; Pankratov, I.; Gun, J. *Anal. Chem.* **1995**, *67*, 22A.
(4) Levy, D.; Esquivias, L. *Adv. Mater.* **1995**, *7*, 120.
(5) Levy, D. *Chem. Mater.* **1997**, *9*, 2666.
(6) Chaumel, F.; Jiang, H.; Kakkar, A. *Chem. Mater.* **2001**, *13*, 3389.
(7) Sayari, A. *Chem. Mater.* **1996**, *8*, 1840.
(8) Corma, A. *Chem. Rev.* **1997**, *97*, 2373.
(9) Blum, J.; Avnir, D.; Schumann, H. *Chemtech* **1999**, 32.
(10) Rodriguez, S. A.; Colon, L. A. *Chem. Mater.* **1999**, *11*, 754.
(11) Iler, R. K. *The Chemistry of Silica*; John Wiley and Sons: New York, 1979.
(12) Koone, N.; Shao, Y.; Zerda, T. W. *J. Phys. Chem.* **1995**, *99*, 16976.
(13) Collinson, M. M.; Howells, A. R. *Anal. Chem.* **2000**, *72*, 702A.
(14) McCain, K. S.; Schluesche, P.; Harris, J. M. *Anal. Chem.* **2004**, *76*, 930.
(15) Meziani, M. J.; Zajax, J.; Jones, D. J.; Partyka, S.; Roziere, J.; Auroux, A. *Langmuir* **2000**, *16*, 2262.
(16) Beck, J. S.; Vartuli, J. C.; Roth, W. J.; Leonowicz, M. R.; Kresge, C. T.; Schmitt, K. D.; Chu, C. T.-W.; Olson, D. H.; Sheppard, E. W.; McCullen, S. B.; Higgins, J. B.; Schlenker, J. L. *J. Am. Chem. Soc.* **1992**, *114*, 10834.
(17) Riversa, D.; Harris, J. M. *Anal. Chem.* **2001**, *73*, 411.
(18) Inaki, Y.; Yoshida, H.; Yoshida, T.; Hattori, T. *J. Phys. Chem. B* **2002**, *106*, 9098.
(19) Higgins, D. A.; Hou, Y. Single Molecule Spectroscopy Studies to Characterize Nanomaterials. *Encyclopedia of Nanoscience and Nanotechnology*; Marcel Dekker: New York, 2004; p 3575.
(20) Moerner, W. E. *Science* **1994**, *265*, 46.
(21) Moerner, W. E. *J. Phys. Chem. B* **2002**, *106*, 910.
(22) Kelley, A. M. Single-Molecule Spectroscopy. In *Encyclopedia of Chemical Physics and Physical Chemistry*; Moore, J. H., Spencer, N. D., Eds.; Institute of Physics Publishing: Bristol, UK, 2001; Vol. 3, p 2199.
(23) Keeking-Tucker, T.; Brennan, J. *Chem. Mater.* **2001**, *13*, 3331.
(24) McCain, K. S.; Hanley, D. C.; Harris, J. M. *Anal. Chem.* **2003**, *75*, 4351.
(25) Wirth, M. J.; Swinton, D. J. *Anal. Chem.* **1998**, *70*, 5264.

10.1021/ja046527j CCC: $27.50

concentrations. The molecules are then located and spectroscopically probed on a molecule-by-molecule basis. Histograms reflecting the shape, width, and average position of the inhomogeneous distribution for the parameter of interest are then prepared. Such methods completely remove the normal ensemble averaging of bulk spectroscopic experiments and allow for much more detailed information on the distribution of microenvironmental properties to be obtained. Details of the underlying distribution of environments become profoundly important when the system under investigation is inhomogeneous.[26−28]

For this paper, SM spectroscopic methods[29,30] were employed to investigate the local acidity of silicate thin films prepared by the sol−gel process. The pH-sensitive fluorescent dye ((5′ and 6′)-carboxy-10-(dimethylamino)-3-hydroxy-spiro[7H-benzo-[*c*]xanthene-7,1′(3H)-isobenzofuran]-3′-one, C.SNARF-1) was employed as the probe.[31−33] A slightly different form of this dye has been employed in previous SM studies of pH in agarose gels.[29] In the present work, the acidity properties of silicate films cast from sols prepared by the acid-catalyzed hydrolysis and condensation of TEOS were studied, along with similar films treated by immersion in different pH solutions. The emission spectra of the C.SNARF-1 molecules were found to clearly reflect the local acidity of the silicate film microenvironments, even in relatively dry films. Fluorescence spectra obtained from a large number of SMs in each sample depict the level of sample heterogeneity in each case. The data are interpreted with regards to the influence of surface silanols and residual catalyst (acid) on the local pH.

Experimental Section

Sample Preparation. Carboxy SNARF-1 (C.SNARF-1) was purchased from Molecular Probes and was used as received. Stock dye solution was prepared using deionized water and was stored in a refrigerator. Sols were prepared by first mixing tetraethoxysilane (TEOS, 2.08 g), absolute ethanol (2.4 mL), water (0.3 mL), and hydrochloric acid (0.5 mL, 0.1 M) in suitable vessels. These mixtures were stirred for 1 h and allowed to stand for 48 h. At the end of this period, C.SNARF-1 was added to each sol to give a final dye concentration in the range of 1−5 nM. The dye-doped sols (in ∼60 μL aliquots) were then spin-cast (6000 rpm, 30 s) onto clean glass microscope coverslips (Fisher Premium) to obtain thin film samples of 300 nm thickness, as measured by surface profilometry. The samples were stored in a desiccator overnight before use. Samples prepared in this manner are designated as "untreated" samples throughout this publication.

The film preparation procedures described above have been employed in several prior publications from our group and are used herein to maintain consistency.[27,28,34] It is well known that the properties of sol−gel silicates can change over long periods of time.[35] Therefore, fixed drying times and drying procedures have been employed to prevent such variables from contributing to the materials properties variations observed. No detectable changes in sample properties were observed during their characterization over relatively brief periods of time (a few hours, at maximum).

To alter the film acidity properties and to explore variations in the accessibility of silicate film microenvironments, the thin films prepared above were also subjected to further treatment by immersion in various pH solutions. For this purpose, solutions of well-defined pH ranging from 3 to 10 were prepared from 50 mM phosphate solutions. The pH in each was adjusted by adding 0.1 M NaOH or HCl. The silicate films were immersed in these solutions (solution volume ≈ 15 mL) for either 1 or 8 h and were then spin-dried. Finally, they were stored in a desiccator overnight before use. These samples are referred to as "treated" samples in the remainder of this paper.

Instrumentation and Methods. A sample scanning confocal microscope was employed in the SM studies and has been described previously.[34,36] Briefly, this system is built upon an inverted, epi-illumination microscope (Nikon). It also incorporates a sample scanning stage (Queensgate) with closed-loop X,Y feedback for precise location and positioning of individual molecules in the detection volume. The 543 nm line from a helium−neon laser was used to excite the dye molecules. A 100X 1.3 numerical aperture oil immersion objective (Nikon) was employed to form a nearly diffraction-limited focus of ∼400-nm $1/e^2$ radius in the sample. The same objective was used to collect fluorescence from the sample and direct it into the detection path. After passage of the fluorescence through a dichroic beam splitter (Omega Optical), residual excitation light was blocked by a holographic notch filter (Kaiser Optical) and band-pass filters (Omega Optical). In imaging experiments, fluorescence from the sample was detected using a single-photon-counting avalanche photodiode (EG&G).

SM fluorescence spectra were obtained by positioning individual molecules in the focal volume of the microscope and sending the collected fluorescence into an imaging spectrograph (Acton Research) and onto a liquid-nitrogen-cooled CCD detector (Princeton Instruments). The spectra were typically integrated for 5 s. Bulk film spectra were acquired from otherwise identical films using a C.SNARF-1 concentration of 100 nM and defocusing the microscope slightly. Bulk solution phase fluorescence spectra were also recorded on this same instrument by placing dye solutions of known pH in a specially designed cell positioned above the microscope objective. Fluorescence from these solutions was excited and detected in a manner identical to that used in the collection of SM fluorescence spectra. The results were compared to similar spectra recorded on a conventional fluorimeter (SPEX).

SM fluorescence intensities near 580 nm (protonated form of C.SNARF-1) and 640 nm (deprotonated form) were obtained by multiplying the individual SM spectra with Gaussian functions centered at 580 and 640 nm (20 nm widths), and integrating the area under each resulting curve. The ratio of these two values was used as a measure of the apparent local pH of the environment surrounding each molecule (see below).

Results and Discussion

Bulk pH Dependence of C.SNARF-1 in Solution. C.SNARF-1 possesses several ionizable functional groups that can be protonated or deprotonated under different pH conditions. Figure 1 shows the chemical structures of the protonated and deprotonated forms of C.SNARF-1 believed to be most relevant to the pH-dependent response of the molecule in the pH 3−10 range.[31]

To better understand the SM fluorescence data, the pH-dependent emission behavior of C.SNARF-1 was first investigated in aqueous solution. Figure 2 shows representative

(26) Hou, Y.; Bardo, A. M.; Martinez, C.; Higgins, D. A. *J. Phys. Chem. B* **2000**, *104*, 212.
(27) Higgins, D. A.; Collinson, M. M.; Saroja, G.; Bardo, A. M. *Chem. Mater.* **2002**, *14*, 3734.
(28) Wang, H.; Bardo, A. M.; Collinson, M. M.; Higgins, D. A. *J. Phys. Chem. B* **1998**, *102*, 7231.
(29) Brasselet, S.; Moerner, W. E. *Single Mol.* **2000**, *1*, 17.
(30) Mason, M. D.; Ray, K.; Pohlers, G.; Cameron, J. F.; Grober, R. D. *J. Phys. Chem. B* **2003**, *107*, 14219.
(31) Whitaker, J. E.; Haugland, R. P.; Prendergast, F. G. *Anal. Biochem.* **1991**, *194*, 330.
(32) Vecer, J. H. A.; Sigler, K. *Photochem. Photobiol.* **2001**, *74*, 8.
(33) Lin, H.-J.; Szmacinski, H.; Lakowicz, J. R. *Anal. Biochem.* **1999**, *269*, 162.
(34) Bardo, A. M.; Collinson, M. M.; Higgins, D. A. *Chem. Mater.* **2001**, *13*, 2713.
(35) Narang, U.; Wang, R.; Prasad, P. N.; Bright, F. V. *J. Phys. Chem.* **1994**, *98*, 17.
(36) Mei, E.; Bardo, A. M.; Collinson, M. M.; Higgins, D. A. *J. Phys. Chem. B* **2000**, *104*, 9973.

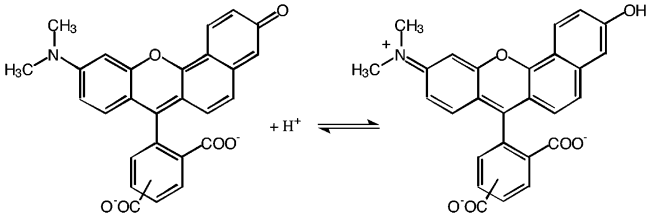

Figure 1. Chemical structures of Carboxy SNARF-1 in its protonated and deprotonated forms.

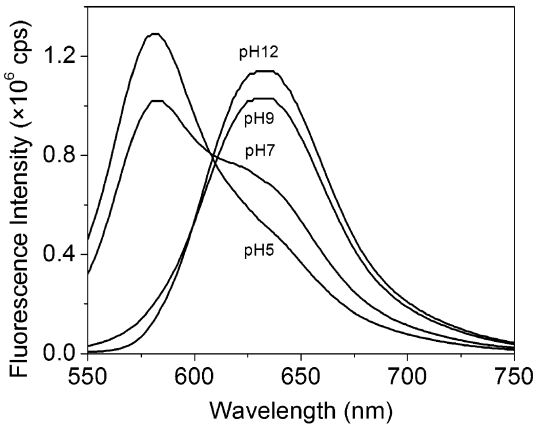

Figure 2. Fluorescence spectra of Carboxy SNARF-1 measured in phosphate solutions of the specified pH. Dye fluorescence was excited using 488 nm light.

fluorescence spectra obtained in bulk spectroscopic experiments performed using a commercial fluorimeter. These data reveal significant pH-dependent changes in the dye's fluorescence spectrum.[31] At low pH, its fluorescence falls predominantly in a band centered near 580 nm. A dramatic decrease in the fluorescence near this wavelength occurs as the pH is increased above 7. Simultaneously, a new emission peak centered near 640 nm grows in (see Figure 2). The spectra also show a clear isoemissive point at 605 nm, pointing to the formation of two distinct species at high and low pH. The ratio, R, of the fluorescence emission at 580 and 640 nm ($R = I_{580}/I_{640}$) can be used as a means to characterize the pH of bulk solutions.[31] The same method has been previously demonstrated to be useful in analyzing SM pH data[29] and is employed for this purpose below.

Quantitatively, the relationship between R and the solution pH is described by the following modified form of the Henderson−Hasselbalch equation.[31]

$$\mathrm{pH} = \mathrm{p}K_a + C \log\left(\frac{R - R_{min}}{R_{max} - R}\right) + \log\left(\frac{I(\mathrm{A})}{I(\mathrm{B})}\right) \qquad (1)$$

In eq 1, R_{min} and R_{max} are the minimum and maximum limiting values of R, and $I(\mathrm{A})/I(\mathrm{B})$ is the ratio of emission intensities for C.SNARF-1 in its acidic (pH 3) and basic (pH 12) forms in solution, at 640 nm. The value of $\log(I(\mathrm{A})/I(\mathrm{B}))$ is small (i.e., −0.4 from the fluorimeter data) for C.SNARF-1 under most circumstances. C is a constant that normally has a magnitude near one. Its sign indicates the relationship between R and pH. In the present case, C is negative, indicating R decreases with increasing pH (see Figure 2). The magnitude of C also serves as an empirical parameter, describing the "slope" of the transition region.[29,31] A large C magnitude indicates a relatively small change in R corresponds to a relatively large change in pH.

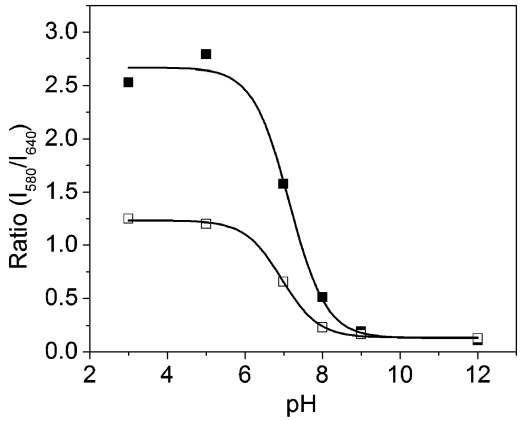

Figure 3. Titration curves depicting the pH-dependent emission ratio (I_{580}/I_{640}) for carboxy SNARF-1 in bulk aqueous solution. ■: bulk spectra obtained from a commercial fluorimeter. □: bulk spectra obtained using the confocal microscope used in the single-molecule experiments.

Figure 3 shows titration curves recorded for bulk pH solutions both on the confocal microscope and in the fluorimeter. The results yield pK_a values for the dye of 7.5 and 7.8, respectively, from eq 1. These closely match the accepted literature values.[31] The values for R, R_{max}, and R_{min} are very sensitive to instrumental parameters such as the wavelength sensitivity of the detection system.[31] As a result, the titration curve obtained on the confocal microscope yields a relatively smaller R_{max} value than does the one obtained from the fluorimeter. However, the R_{min} values are similar, as are the C values. All such parameters for the bulk (and SM) data are given in Table 1. Finally, the $\log(I(\mathrm{A})/I(\mathrm{B}))$ value obtained from the microscope data is also very similar to that obtained using the fluorimeter (−0.5 vs −0.4). All SM data described below are interpreted on the basis of bulk results obtained using the confocal microscope and identical optics and filter sets. Therefore, no spectral corrections need be applied prior to estimating the local pH from the SM data. Because $\log(I(\mathrm{A})/I(\mathrm{B}))$ was found to be small in both cases above, and because of the difficulties in determining its value in SM studies of thin films, it was simply set to zero in analyzing all data from thin film samples.

Fluorescence Images of C.SNARF-1-Doped Silicate Films. Typical images of silicate thin films doped with C.SNARF-1 at nanomolar levels are presented in Figure 4. Both the untreated (Figure 4A) and the treated samples (Figure 4B,C) show several round fluorescent spots in their respective images. The well-separated bright spots represent fluorescence emission by single dye molecules, as deduced from the discrete photobleaching and blinking events observed in the images.[34] Such images were recorded primarily for the purpose of locating the SMs for later spectral analysis. However, they also show that the immersion treatment does not significantly alter the samples. Specifically, sufficient numbers of molecules remain in the films even after treatment for up to 8 h.

SM Fluorescence Data from Untreated Films. Fluorescence spectra for single C.SNARF-1 molecules were obtained by positioning the individual dye molecules (one at a time) within the excitation volume of the microscope and recording their spectra using a spectrograph and CCD (see Experimental Section for details). In all such experiments, and for a variety of samples, various spectral peak shapes and diverse emission positions were observed, even for different molecules in the same film. These

Table 1. Parameters Derived from Fitting of Bulk and SM Titration Curves to Eq 1

	soln[a]	soln[b]	SM 8 h	bulk 8 h	SM 1 h	bulk 1 h	bulk[c] 4 h
R_{max}	1.23	2.67	1.17	1.40	1.22	1.37	1.30
R_{min}	0.14	0.13	0.79	0.84	0.84	0.91	0.94
pK_a [d]	7.5	7.8	7.2	7.3	7.1	7.3	7.6
C	−1.30	−1.14	−0.79	−0.62	−1.42	−1.88	−0.83

[a] Bulk solution data obtained using the confocal microscope. [b] Bulk solution data obtained using the commercial fluorimeter. [c] Bulk film data obtained using the confocal microscope. [d] Calculation of the pK_a values for bulk solutions employed the $\log(I(A)/I(B))$ ratios given in the text. All pK_a's determined from thin films were obtained by setting this parameter to zero.

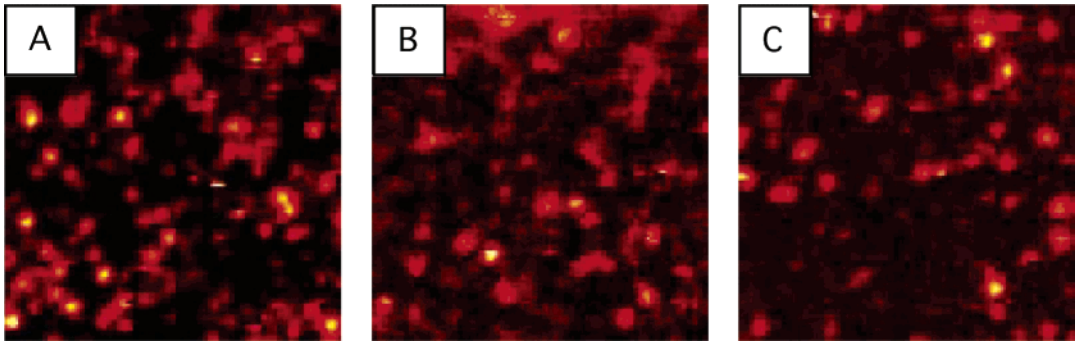

Figure 4. Fluorescence images (10 × 10 μm) of C.SNARF-1-doped silicate films. (A) Untreated TEOS film. (B, C) TEOS films treated for 8 h in pH 10 and pH 3 solutions, respectively.

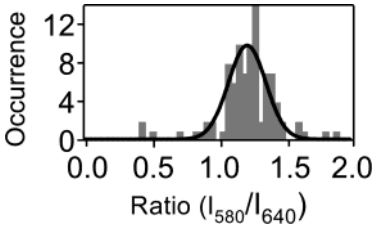

Figure 5. Histogram of emission intensity ratio ($R = I_{580}/I_{640}$) for untreated C.SNARF-1-doped silicate films. The approximate mean value of R is 1.20, and the distribution width, 2σ, is 0.27.

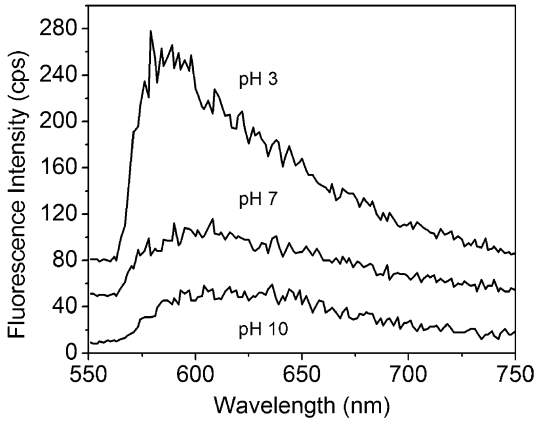

Figure 6. Representative SM fluorescence spectra obtained from the doped films after treatment at the specified pH.

results indicate that substantial nanoscale heterogeneity in the acidity properties of these films exists under many circumstances.

A histogram of the R values obtained from numerous SMs in the untreated films is presented in Figure 5. The approximate peak position and width for each inhomogeneous distribution are determined by fitting the histogram data to a Gaussian profile. The peak position determined in this manner provides a measure of the average acidity of the local environments found. For the untreated samples, a value of 1.2 is obtained, reflecting an average local pH of ∼4.8. C.SNARF-1 is present primarily in its protonated form in this sample, and the film environments are, on average, slightly acidic. Such information could have been readily obtained from bulk spectroscopic studies. However, the use of SM data provides much more information, particularly associated with the range and prevalence of different environments present. Such information is difficult to obtain by any other means.

The width of the distribution shown in Figure 5 is approximately 0.27 (2σ). Although it is not yet certain that such spectral variability results from variations in environment acidity (see below), comparison to the solution data suggests a lower bound of about 1−2 pH units can be placed on the pH range of the associated environments. The local acidity in silicate films prepared by the acid-catalyzed hydrolysis and condensation of TEOS likely varies with local variations in the concentration of residual HCl. Variations in the local acidity may also arise from variations in the local density of surface silanols and their pK_a values.

The heterogeneity reflected in these data (Figure 5) appears to be predominantly static. Up to 15 sequential spectra (2 s integration time) recorded for several individual molecules yielded an average variability in R of 0.07 (2σ), equivalent to $\sim^1/_4$ of the histogram width in Figure 5. Hence, the observed heterogeneity may be concluded to result from site-to-site (i.e., positional, rather than temporal) variations in the local acidity, at least on a tens-of-seconds time scale.

SM Fluorescence Data from Treated Films. Data acquired from the immersion treated films provides important information on the sensitivity of the SM data to actual variations in local matrix acidity. Representative SM spectra obtained from the treated films are presented in Figure 6. All such spectra are truncated on the blue end by the filters employed. This does not alter the apparent local pH determined from the data. Identical filter sets were employed in the recording of all bulk data on the microscope, to which the SM data are compared for assignment of the local pH. For films treated at low pH,

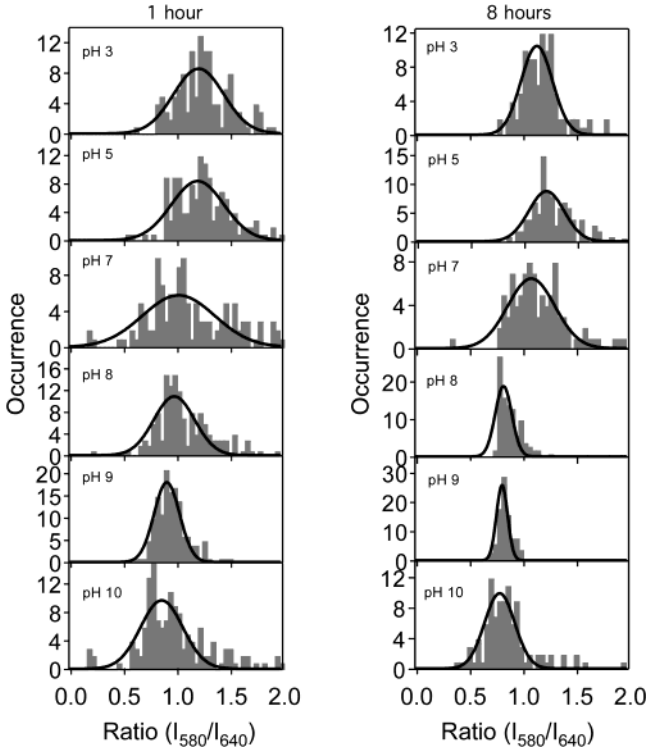

Figure 7. Histograms of the emission intensity ratio ($R = I_{580}/I_{640}$) for silicate films treated at the specified pH. Left: Films treated by immersion for 1 h. Right: Films treated by immersion for 8 h. The C.SNARF-1 concentration in the final sol was ~5 nM.

individual molecules were found to exhibit emission maxima around 580 nm, as expected for protonated C.SNARF-1. In contrast, films treated with basic solutions led to a clear predominance of fluorescence near 640 nm, consistent with emission by deprotonated C.SNARF-1. At intermediate pH, the spectra take on an intermediate appearance, consistent with the effects of rapid proton exchange between the dye molecules and their surrounding environment (i.e., they are in dynamic equilibrium). A noticeable decrease in the SM emission intensity was also observed for films treated at high pH, suggesting that SM data obtained using C.SNARF-1 might be biased toward acidic film environments. Such a bias would arise because the brightest fluorescent spots in an image would be most often selected for further characterization (see below).

Histograms depicting the distribution of emission ratios, *R*, for the treated samples are shown in Figure 7. Data are shown for films immersed in different pH solutions for periods of 1 and 8 h. Each histogram contains data from more than 100 molecules. The approximate mean values and widths for these distributions were determined by fitting each to a single Gaussian function. The mean values of *R* are presented in Figure 8 as a function of treatment pH; the widths of the distributions are presented in Figure 9.

There are clear differences between the histograms obtained following 1 and 8 h treatments. The distributions obtained after 8 h most clearly depict changes in the sample environments induced by the treatment procedure. They also exhibit more profound variations as a function of treatment pH. As a result, these latter data provide the best evidence that the SM data indeed provide a sensitive measure of local film acidity. Data from the samples treated for 8 h will be discussed first, as a means to demonstrate this sensitivity.

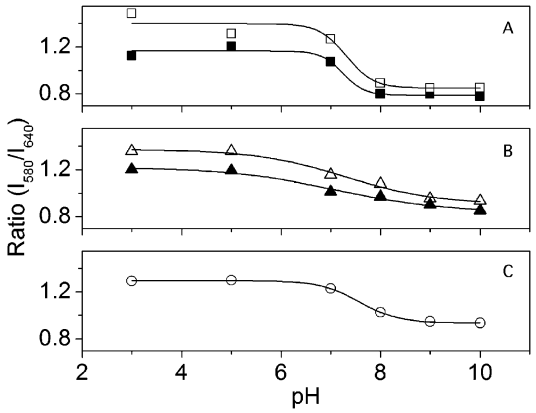

Figure 8. Titration curves derived from the SM data obtained from (A) 8 and (B) 1 h treated samples, respectively, and (C) bulk fluorescence of C.SNARF-1 in silicate films treated for 4 h. Filled symbols depict the emission intensity ratios obtained from the mean of each distribution shown in Figure 7, while the open symbols depict those obtained by summing all SM spectra used in the construction of the Figure 7 histograms to produce "simulated" bulk spectra.

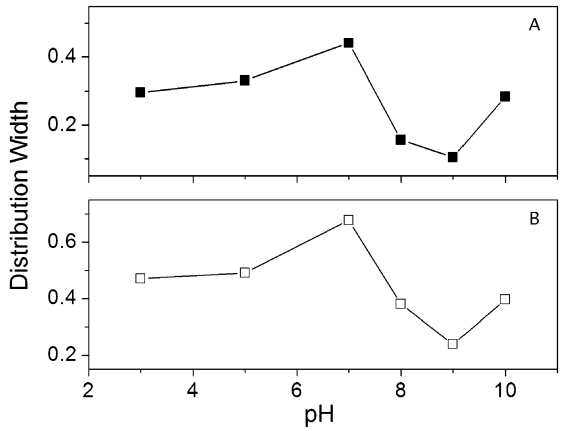

Figure 9. Widths, 2σ, of the histograms shown in Figure 7. Width data are shown for both (A) 8 and (B) 1 h treated samples.

The mean *R* values obtained from these (8 h) films yield a titration curve that mimics the bulk solution titration curve (compare Figures 3 and 8). The titration curve also gives a similar pK_a value for the dye (see Table 1). Again, pK_a calculations from the bulk solutions incorporate a small but nonzero log(I(A)/I(B)), while this value is set to zero in all calculations based on thin film data. In contrast, R_{max} determined from the SM data is somewhat smaller and R_{min} is somewhat larger than those in the bulk solution data (see Table 1). *C* also differs for the 8 h SM data. Such variations likely arise from entrapment of some of the molecules in inaccessible pores within the film (see below). The environments within the films are also relatively dry as compared to bulk aqueous solution. As a result, some changes in the spectroscopic properties of the dye are expected. Despite these differences, the pH dependence observed for the mean *R* values (see Figure 8) proves that the dye remains sensitive to the local matrix acidity, even in relatively dry films.

The histogram widths provide another means for assessing the pH sensitivity of the SM data. Some of the histograms depicted in Figure 7 are quite broad. The breadth of these distributions may arise from variations in local matrix acidity, or they may result from variations in a number of other physical and chemical parameters associated with the nanoscale environment in which each molecule is entrapped. For example,

entrapment of certain molecules in confined environments may result in "rigidochromic" shifts in their emission spectra.[37,38] Molecules entrapped in environments of different polarities may also exhibit profound spectral shifts.[26,27,34,39,40]

Here, it is shown that the spectral variability reflected in the histogram widths is most likely due to site-to-site variations in local acidity. Some of the strongest supporting evidence is provided by the dramatic, reproducible, pH-dependent variations in the histogram widths obtained for the 8 h treated films (see Figures 7 and 9). The histograms are relatively wide for samples treated at pH 3 and 5, but the broadest histograms are obtained for films treated in pH 7 solutions. A dramatic decrease in the distribution width is then observed for films treated at pH 8 and 9, followed by a subsequent increase in width for films treated at pH 10.

The greatly increased width of the distributions observed for pH 7 films provides strong evidence for the pH sensitivity of the SM spectra. In these samples, the average pH of the microenvironments is very close to the pK_a of C.SNARF-1. The dye is most sensitive to variations in the local acidity in this pH range, and, hence, the largest distribution width is observed.[29] These data are consistent with small changes in the local acidity causing dramatic shifts in R near pH 7.

The significant decrease in the distribution width at pH 8 and 9, for which $2\sigma = 0.15$ and 0.10, respectively, is attributable to the buffering effects of the surface silanols. The majority of silanol species found on silica surfaces have been previously assigned pK_a values of 8.5−9.[11,41] These silanols serve as sinks/sources for hydrogen ions in the corresponding pH range, making the film environments much more homogeneous in terms of the local pH. Note that the observed narrowing of the distributions at pH 8 and 9 cannot be explained by the buffering effects of the treatment solutions because the pK_a values of phosphoric acid are not in this range. The widths of the pH 8 and 9 histograms obtained after 8 h treatment then provide an estimate of the minimum distribution width expected for films of uniform pH. In this case, the width would be reflective of random errors in the measurement of R. Alternatively, one may assume the widths at pH 8 and 9 represent an upper bound for the contributions made by variations in the silanol pK_a values (and other physical phenomena) to the distribution widths. It may then be concluded that the broader distributions obtained at different pH values result primarily from variations in the acid or base content of the film microenvironments following the treatment procedure.

Comparison of the histogram data obtained from the samples treated for 1 and 8 h provides detailed information on the different acidity properties of these two sets of samples. These data also provide important information on the solvent accessibility of the different microenvironments in each film. In general, the distributions are significantly broader for the films treated for only 1 h, indicating the acidity properties of the 1 h treated films are much more heterogeneous. Such comparisons could not readily have been made using bulk spectroscopic data. Longer immersion times in general result in narrower distributions in the R values obtained. Such observations represent clear evidence for kinetic limitation of the environmental acidity properties. Some of the pores in these films are likely to be inaccessible to the immersion solutions on time scales ≤ 1 h. With longer immersion time, the acidity properties of the microenvironments are controlled to a greater extent by the immersion solution.

The R distributions for the samples treated for 1 h indicate that some SMs remain protonated, even after treatment at high pH. The presence of such molecules is reflected by R values greater than 1.0 for the films treated at pH 10. However, some SMs in these same films also yield R values of 0.7 and smaller, a clear indication that these molecules tend to be deprotonated. Similar results are obtained at even higher pH. These results have not been included because the films are believed to be unstable due to instability of the siloxane bonds at high pH. At low pH, the distributions reflect the presence of microenvironments having greater than the expected pH, while others are closer to what is expected following exposure to the treatment solutions. These results are a clear indication that on a 1-h time scale some of the molecules are completely inaccessible to external solutions, while others are at least partially accessible. The inaccessible molecules are likely entrapped within tightly confined pores deep within these films. In such environments, the concentration of residual HCl likely plays a dominant role in governing the local pH.

As shown in Figures 7 and 8, the average acidity properties of the films treated for 1 h do indeed change as a function of treatment pH. However, the trend is not as dramatic as in either the bulk solution data or that obtained from the samples treated for 8 h. Table 1 presents the relevant parameters obtained by fitting the titration curves. This apparent reduction in pH sensitivity of the dye can be explained entirely by the entrapment of a subset of molecules in solvent inaccessible microenvironments. Clearly, for shorter treatment times, the acidity of the film, as reflected by the spectroscopic data, more closely mimics the properties of the untreated film. As the overall (or average) response of the material is derived from the responses of all of the individual molecules, the presence of molecules entrapped in "static" (inaccessible) microenvironments leads to a more gradual pH-dependent response than is observed in bulk solutions. This result is particularly relevant to applications of sol−gel-derived materials as chemical sensors. Entrapment of molecules in inaccessible environments reduces the sensitivity of such devices, especially on short time scales. On longer time scales (8 h), the majority of such environments become accessible and the sensitivity to a change in pH increases.

Comparison to Bulk Film Results. Figure 8 plots titration curves derived from bulk spectroscopic data, along with those obtained from the SM results. True bulk data are plotted in Figure 8C for silicate films similar to those used in the SM studies, while "simulated" bulk data obtained by summing the individual SM spectra are plotted in Figure 8A and B (open symbols). The true bulk data were obtained from films treated for an intermediate length of time (4 h). Again, these data were obtained from films containing a relatively high concentration of dye by defocusing the microscope. This titration curve closely mimics those obtained from the SM results, but is shifted slightly to higher R values (see Table 1). The transition region is also shifted toward higher pH, as reflected by a shift in the apparent

(37) Wrighton, M.; Morse, D. L. *J. Am. Chem. Soc.* **1974**, *96*, 998.
(38) McKiernan, J.; Pouxviel, J.-C.; Dunn, B.; Zink, J. I. *J. Phys. Chem.* **1989**, *93*, 2129.
(39) Brunschwig, B. S.; Ehrenson, S.; Sutin, N. *J. Phys. Chem.* **1987**, *91*, 4714.
(40) Reichardt, C. *Chem. Rev.* **1994**, *94*, 2319.
(41) Ong, S.; Zhao, X.; Eisenthal, K. B. *Chem. Phys. Lett.* **1992**, *191*, 327.

pK_a. The increase in measured R values results from the different weightings given to each spectrum in the SM and bulk data. In the SM histograms, each molecule carries equal weight and contributes equally to the determination of R at each pH, regardless of its emission intensity. In contrast, R values derived from bulk data are weighted by the intensity of the molecular emission. Because the C.SNARF-1 molecules are observed to be more fluorescent in acidic environments, they contribute to a greater extent to the bulk spectra. Hence, the R value measured at each pH is higher in the bulk data.

Biasing of the bulk results to higher R values is also evidenced in the "simulated" bulk data (obtained by summing the SM spectra) shown in Figure 8A and B (open symbols). In both cases (8 and 1 h data), the titration curves obtained are shifted to higher R values as compared to the SM results, especially at low pH. It is also particularly noteworthy that the R_{max} values from the "simulated" bulk data are both larger than that of the true bulk data (see Table 1). Such observations are consistent with the slight biasing of the SM results toward more fluorescent molecules in the more acidic environments, as mentioned above.

The different weightings given to the individual molecules in the bulk and SM data also lead to the observation of different apparent pK_a values for the dye molecule. The bulk film data all yield significantly higher pK_a values for C.SNARF-1 because of the greater contributions of molecules in acidic environments to the spectra. Again, in the SM results, each molecule is weighted equally in the R determinations, regardless of its emission intensity. As a result, there is potentially less error due to quantum yield and excitation cross-section variations in the SM results than in raw bulk data. Baring significant errors due to biased selection of more fluorescent SMs, the pK_a results obtained from SM data should then better reflect the true pK_a of the dye. Because of the difficulties associated with correcting bulk film fluorescence data for such photophysical properties variations, SM measurements may then provide a more accurate view of the average pH of the local environments within thin films, as well as providing a much more complete picture of the site-to-site variations in local pH.

One important application of sol−gel-derived materials in analytical science has been the development of chemical sensors.[1,3,42] In these investigations, a suitable receptor is added to a sol, which upon gelation traps the receptor into what is ideally a "porous" host.[1,3,42] Of utmost concern in the development of viable chemical sensors using sol−gel processing is the accessibility of an external reagent to an immobilized receptor. This accessibility dictates response times, recovery rates, and the presence or absence of hysteresis in repetitive measurements.[1,3,42] Many studies have utilized thin films as the sensing platform.[1,3,42] While the path length for diffusion is smaller in thin films relative to bulk gels, thin films can be significantly less porous due to the manner in which they are prepared.[43] As a result, questions are often raised about how truly accessible the immobilized receptors are to an external reagent.

Previous work on sol−gel-derived pH sensors in particular has shown broad titration curves. These have been attributed primarily to site heterogeneity and a distribution of pK_a values for the immobilized dye molecules.[44−51] While this may be true, it does not represent the entire story. Figure 8 clearly shows that the titration curve breadth is also influenced by the length of time the film is immersed in solutions of varying pH. In previous work, response times were believed to be seconds to minutes.[44−51] This apparently is not sufficient to truly access all sites within a film. In previous work by Saavedra and coworkers, significant hysteresis was observed for the first few cycles of changing the pH of the solution for sol−gel entrapped bromocresol purple films.[44] They conjectured that this "may be caused by a subpopulation of indicator molecules that respond to solution pH changes more slowly than the remainder of the population."[44] Our work clearly supports this statement and brings attention to the fact that not all sites in these materials are equivalent.

Conclusions

In summary, single-molecule spectroscopic methods have been employed for the first time to study the acidity properties of the microenvironments present in silicate thin films. The emission characteristics observed for individual dye molecules were shown to provide a sensitive means for assessing both average film acidity and the distribution of microenvironment acidity properties, even in relatively dry films. Single-molecule fluorescence spectra obtained in these studies varied from molecule to molecule, reflecting a significant level of sample heterogeneity. Proof that these spectral variations arose primarily from site-to-site variations in local acidity was derived from the pH-dependent histogram widths. The histograms became markedly narrower as the film treatment pH approached the pK_a of the most common silanol sites, as a result of their buffering capabilities. The dramatic increase in histogram width observed for films treated at pH values near the pK_a of the dye provided further evidence. Studies performed as a function of treatment time demonstrate that kinetic factors limited the pH response of many of the single molecules. Specifically, these results confirm[49] that many silicate microenvironments are inaccessible to external solutions on time scales as long as 1 h. However, the majority of microenvironments were accessible to the treatment solutions when exposed for time scales approaching 8 h. Such kinetic limits to the sensitivity of these materials are of importance to those developing chemical sensors from sol−gel-derived silicate films and will be particularly relevant to those seeking to produce better pH sensors.

Acknowledgment. We thank the National Science Foundation (CHE-0316466) for support of this research.

JA046527J

(42) Wolfbeis, O. S.; Reisfeld, R.; Oehme, I. *Struct. Bonding* **1996**, *85*, 51.
(43) Frye, G. C.; Ricco, A. J.; Martin, S. J.; Brinker, C. J. *Mater. Res. Soc. Symp. Proc.* **1988**, *121*, 349.
(44) Yang, L.; Saavedra, S. S. *Anal. Chem.* **1995**, *67*, 1307.
(45) Browne, C. A.; Tarrant, D. H.; Olteanu, M. S.; Mullens, J. W.; Chronister, E. L. *Anal. Chem.* **1996**, *68*, 2289.
(46) Nguyen, T.; McNamara, K. P.; Rosenzweig, A. *Anal. Chim. Acta* **1999**, *400*, 45.
(47) Lacan, P.; Le Gall, P.; Rigola, J.; Lurin, C.; Wettling, D.; Guizard, C.; Cort, L. *Proc. SPIE* **1992**, *1758*, 464.
(48) Kraus, S. C.; Czolk, R.; Reichert, J.; Ache, H. J. *Sens. Actuators* **1993**, *15−16*, 199.
(49) Lee, J. E.; Saavedra, S. S. *Anal. Chim. Acta* **1994**, *285*, 265.
(50) Makote, R.; Collinson, M. M. *Anal. Chim. Acta* **1999**, *394*, 195.
(51) Lobnik, A.; Oehme, I.; Murkovic, I.; Wolfbeis, O. S. *Anal. Chim. Acta* **1998**, *367*, 159.